[AMERICAN JOURNAL OF SCIENCE, VOL. 279, FEBRUARY, 1979, P. 129-160]

# STRUCTURAL AND CHEMICAL ASPECTS OF METAMORPHIC LAYERING DEVELOPMENT IN METASEDIMENTS FROM CLUNES, AUSTRALIA

MICHAEL B. STEPHENS*, MICHAEL J. GLASSON, and REID R. KEAYS

Department of Geology, School of Earth Sciences, University of Melbourne, Parkville, Victoria 3052, Australia

ABSTRACT. The microstructure, whole rock, and phyllosilicate chemistry of a sequence of slightly metamorphosed sandstones, laminated siltstones, and pelites from Clunes, Victoria, Australia are described, and a model is presented for the development of the metamorphic layering ($S_1$) which forms an axial surface structure to meso- and microfolds in bedding ($S_0$). The metamorphic layering is defined by relative concentrations of white mica + chlorite (P-layers) and quartz (Q-layers). The development of P-layers is fold-dependent in the laminated siltstones and pelites but remains prominent in the sandstones even though folding is generally absent.

Solution-mica precipitation and ion exchange reactions between pre-$S_1$ (detrital and diagenetic) phyllosilicates and the ambient pore fluid occurred in both P- and Q-layers but appear to have been more significant in the P-layers. In particular, the rate of ion exchange reactions was promoted along the P-layers due both to increased diffusivity of ionic species within and between pre-$S_1$ grains. Relative to the composition of the Q-layers and on the basis that Ti neither left nor was added to the system, there were considerable ($\geqslant$40 percent) losses of Na, Si, Mn, and Ca, smaller (15 to 40 percent) losses of P, total Fe, volatiles, Mg, and Al, minor (<15 percent) losses of Zr and Y, and minor, (<15 percent) addition of K during P-layer formation. The material lost is thought to have left the local system along the P-layers, probably to be deposited in quartz ($\pm$ chlorite) and carbonate veins. A minimum estimate for the net loss in volume during formation of $S_1$ is in the order 10 to 20 percent of the original rock volume.

In the foliation model the dark P-layers correspond to zones of relatively high permeability established during the early strain increments of $D_1$ due to the modification of existing pore shapes. Expulsion of trapped pore fluid and attendant reactions (dissolution, ion exchange) between the fluid and pre-$S_1$ mineral grains occurred during later stages of $D_1$ particularly along the incipient P-layers. Dissolution of albite, quartz, pre-$S_1$ chlorite, diagenetic carbonate, and probably also pre-$S_1$ white mica are consistent with the chemical data. Precipitation and growth of new phengite mica, in equilibrium with the fluid, accompanied these reactions and formed by the removal from the fluid of Si, K, and to a less extent Fe and Mg and combination with Al readily available in the rock. Availability of K in the fluid was the critical factor determining the amount of new phengitic mica produced, minor addition of mica actually occurring along the P-layers. The preferred orientation of the new micas parallel to the layering was largely controlled by the anisotropic supply of constituent material to the faces of newly precipitated grains (Etheridge, Paterson, and Hobbs, 1974), that is, the permeability of the system during $D_1$. Although differentiation into P- and Q-layers is intrinsically related to the establishment of relatively high and low permeability zones, the present character of the layers is determined by the more pronounced chemical changes that occurred along the high permeability zones.

It is considered that the extreme mineralogical and chemical differences between adjacent P- and Q-layers and the variable $S_1$ morphology in different lithologies raise the question of whether the mechanism of pressure solution is solely responsible for the greater dissolution and precipitation of material along the incipient P-layers. It is suggested that the differentiation into P- and Q-layers is related to the faster rate of dissolution and mica precipitation reactions along the incipient P-layers, due to enhanced fluid flow along these high permeability zones. Such a model may be acting quite independently of or at the same time as pressure solution effects.

* Present address: Geological Survey of Sweden, Fack, 104 05 Stockholm 50, Sweden

## INTRODUCTION

Discussion of axial surface foliations in the literature has been largely concerned with three problems:

1. nomenclature;
2. mechanisms involved in their formation;
3. relationship between the foliation and the finite strain ellipsoid.

Attempts to define a practical terminology for such foliations (for example, Knill, 1960; Rickard, 1961; Talbot and Hobbs, 1968; Ramsay, 1967, p. 177; Cosgrove, 1976) have tended to obscure the overlapping nature of their morphology and, thus, their possibly related origins. The gradation in morphology of many types of axial surface foliation appears to indicate that several mechanisms are important in their development, but under different physico-chemical conditions one or more mechanisms may be effective in defining a particular foliation. Factors such as the presence of an initial anisotropy, the relative timing of foliation development in a deformation-metamorphic sequence, the presence or absence of a pore fluid, and the PT conditions of deformation and metamorphism will control which mechanism or combination of mechanisms is the most important. A similar viewpoint has also been expressed by Helm and Siddans (1971) and Wood (1974) with respect to slaty cleavage. It is considered that an understanding of both the strain history and the mechanism(s) involved in the formation of a particular foliation are a prerequisite for any prediction concerning the relationship between the foliation and the finite strain ellipsoid.

Several processes have been suggested as an explanation for axial surface foliation development. These include:

1. mechanical rotation of inequidimensional particles due to either finite strain (Sorby, 1856; Means and Paterson, 1966; Oertel, 1970; Williams, 1972) or the passage of fluid through relatively unconsolidated sediment under the influence of high pore fluid pressure (Maxwell, 1962; Powell, 1969);

2. deformation of preexisting grains or objects including, for example, individual quartz grains (Wilson, 1973), ooliths (Cloos, 1947), or pebbles (Hossack, 1968; Gay, 1969; Stephens, 1975);

3. differential solution and precipitation of material during deformation (Plessmann, 1964; Durney, 1972; Williams, 1972; Elliot, 1973; Groshong, 1975; Cosgrove, 1976; Gray, 1977);

4. stress and/or strain induced recrystallization (Green, Griggs, and Christie, 1970) and/or mineral grain growth (Kamb, 1959) including the orientation-dependent growth mechanisms of Etheridge, Paterson, and Hobbs (1974).

The present study is concerned with the development of axial surface foliation in slightly metamorphosed sandstones, siltstones, and pelites in boreholes from the Clunes goldfield, central Victoria, Australia. The study was initiated in connection with a project aimed at assessing the relationship between cleavage development and gold deposits in the

Victorian slate belt (Glasson and Keays, 1978). The microstructure, bulk rock chemistry, and phyllosilicate chemistry of these rocks are described in detail. The results demonstrate that in this particular low-grade environment the foliation developed by a complex interaction of mechanical and chemical processes. It is suggested that the processes of recrystallization and/or mineral grain growth, although apparently the dominant mechanism of preferred orientation development in many deformed rocks, obscure the earlier deformation history and lead to an oversimplified picture of foliation development.

## GEOLOGICAL SETTING

Clunes lies approx 110 km west-northwest of Melbourne (fig. 1) and forms the center of a goldfield worked during the latter half of the last century. The Clunes goldfield is situated geologically in the auriferous slate belt of central Victoria. Northwest of Melbourne the slate belt is composed of Ordovician and possibly older graywackes, siltstones, shales, and slates (Singleton, 1965). The sandy beds are often graded, alternate with the finer pelitic units, and thought by Hills and Thomas (1954) to have been deposited from turbidity currents.

The bedrock around Clunes is an alternating series of sandstones, siltstones, and pelites which have been assigned a Lower Ordovician age (Coldham, 1953); exposure of these rocks is limited to an area adjacent to Creswick Creek which flows through the Clunes township (fig. 1). The Lower Ordovician rocks are overlain by Tertiary alluvial sediments and/or later basalt flows. A few kilometers to the west of Clunes a granite body of Lower Devonian age forms a series of peaks rising above the basalt plain. Various acidic and doleritic dikes have been located in the old mine workings (Baragwanath, 1917) and in more recent diamond drill holes.

Macroscopically the Ordovician rocks at Clunes are folded about a tight anticline which trends 10° east of north and plunges gently to north and south (Coldham, 1953; and fig. 1); the old mine workings are located along the axial surface trace of the anticline (fig. 1). This fold conforms to the macroscopic structural pattern of the Ordovician rocks in central Victoria (Thomas, 1939). A description of the mesoscopic structures within the Ordovician of Victoria has been presented by Beavis (1967).

The samples used in this study were collected from three inclined diamond drill holes which penetrated both limbs of the anticline. The locations of the drill holes are indicated on figure 1.

## PETROGRAPHY AND MESOSCOPIC STRUCTURE

The drill cores consist of an alternation of three main lithologies.

1. Fine to medium grained, poorly sorted sandstones are composed predominantly of quartz, albite (10 percent and above), white mica, and chlorite with accessory amounts of pyrite, zircon, tourmaline, and Ti-rich minerals; chert and pelite lithic fragments and sideritic carbonate

are present in some sandstones. The carbonate occurs either as ellipsoidal blebs, ranging from 0.3 to 2 mm across in sections perpendicular to the axial surface foliation, or in veins. Sideritic carbonate blebs are often concentrated either along sandstone-pelite contacts or around pelite clasts, while the carbonate veins lie parallel to and cut across the axial surface foliation. The sideritic carbonate provides a clear example of mobility of material both during early post-depositional modification of the sandstones (formation of blebs) and during foliation development (formation of veins).

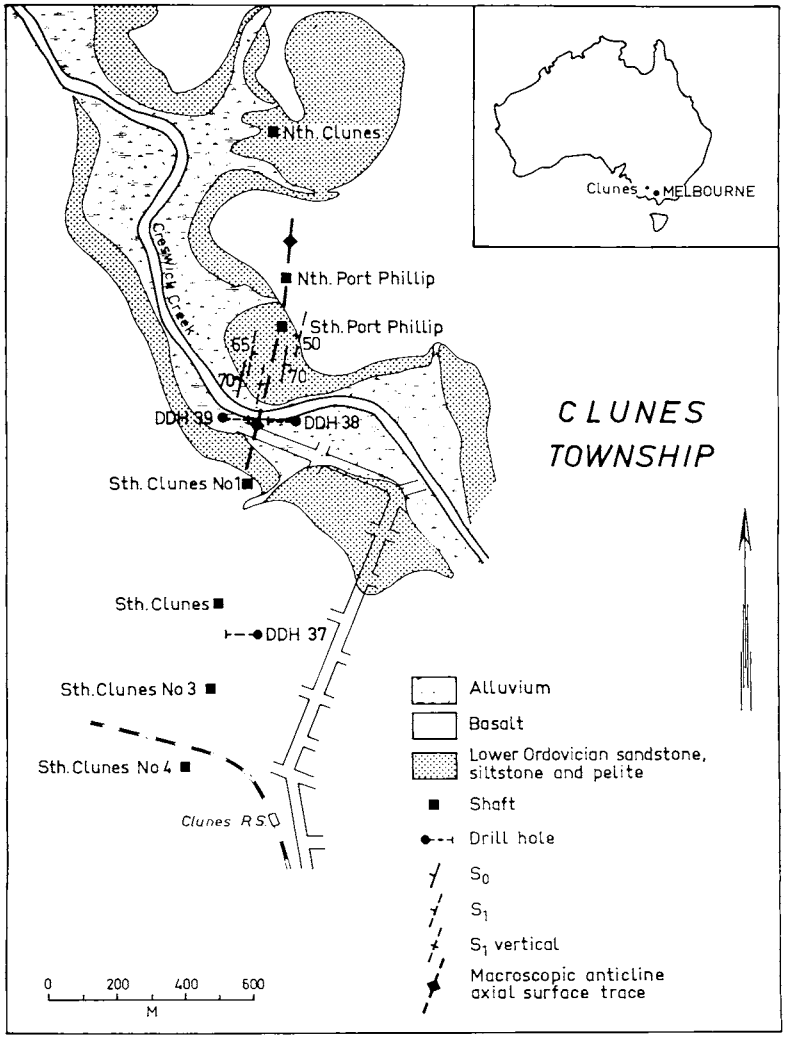


Fig. 1. General geology and location of drill holes at Clunes.

2. Laminated units of siltstone and/or siltstone and fine sandstone exhibit the same mineralogy as the sandstones, but there is a higher proportion of phyllosilicates compared to quartz and feldspar.

3. Gray-green to black pelites are subordinate to the sandstones and siltstones. They are composed of the same minerals as the sandstones but are dominated by phyllosilicates; detrital quartz grains are less than 10 $\mu$m across.

The structure within these lithologies can be conveniently divided into two groups separated by their geometrical relationships to the bedding ($S_0$) and axial surface foliation ($S_1$). $S_1$ formed during the single phase of deformation ($D_1$) which has affected these rocks.

Group 1 structures are either enclosed between or defined along the $S_0$ surfaces and are transected by $S_1$, that is, they predate the axial surface foliation; these include graded bedding, intrastratal folding (slumping and minor bedding irregularities), cross-lamination, and occasional load casts associated with highly irregular flame structures. In some siltstones and fine sandstones the cross-laminations are steepened and even overturned; these steepened foresets are unambiguously deformed and crosscut by $S_1$. Such structures are common in water-saturated sediments (McKee, Reynolds, and Baker, 1962; Allen and Banks, 1972; Lowe, 1974), and their formation has been related to the escape of trapped pore fluid during sedimentation and/or the initial stages of consolidation.

The group 2 structures include $F_1$ mesoscopic folds (pl. 1-A) parasitic to the macroscopic anticline and mullions (pl. 1-B and Beavis, 1970); these structures deform $S_0$ and contain $S_1$ as an axial surface structure. The mullions are distinct from load casts in that:

1. They occasionally occur at the top as well as at the base of ungraded sandstone units (see also Beavis, 1970).

2. The $S_1$ foliation converges inward toward the tightly pinched fold between the sandstone mullions, thus determining a regular relationship between $S_1$ and the mullion shape (pl. 1-B).

Other structures included in group 2 are isolated lobes of sandstone, often within pelite and around which $S_1$ wraps without any crosscutting relationship (pl. 1-C), and irregular lozenges of fine sandstone strung out within $S_1$ which is developed in the surrounding silty material (pl. 1-D).

Since $S_1$ forms an axial surface structure to the $F_1$ mesoscopic folds and the mullions, it is considered that both folds and mullions formed at approximately the same time as $S_1$. The sandstone lobes possess sharp bases and necked, diffuse tops and often occur beneath irregular sandstone over pelite contacts. This structure corresponds to the "lobate bedding" of Hills (1963); similar structures have been described from the Martinsburg shale by Alterman (1973). Since the sandstone lobes appear to grade spatially into the mullions, it is suggested that the former are also syn-$S_1$ structures.

PLATE 1

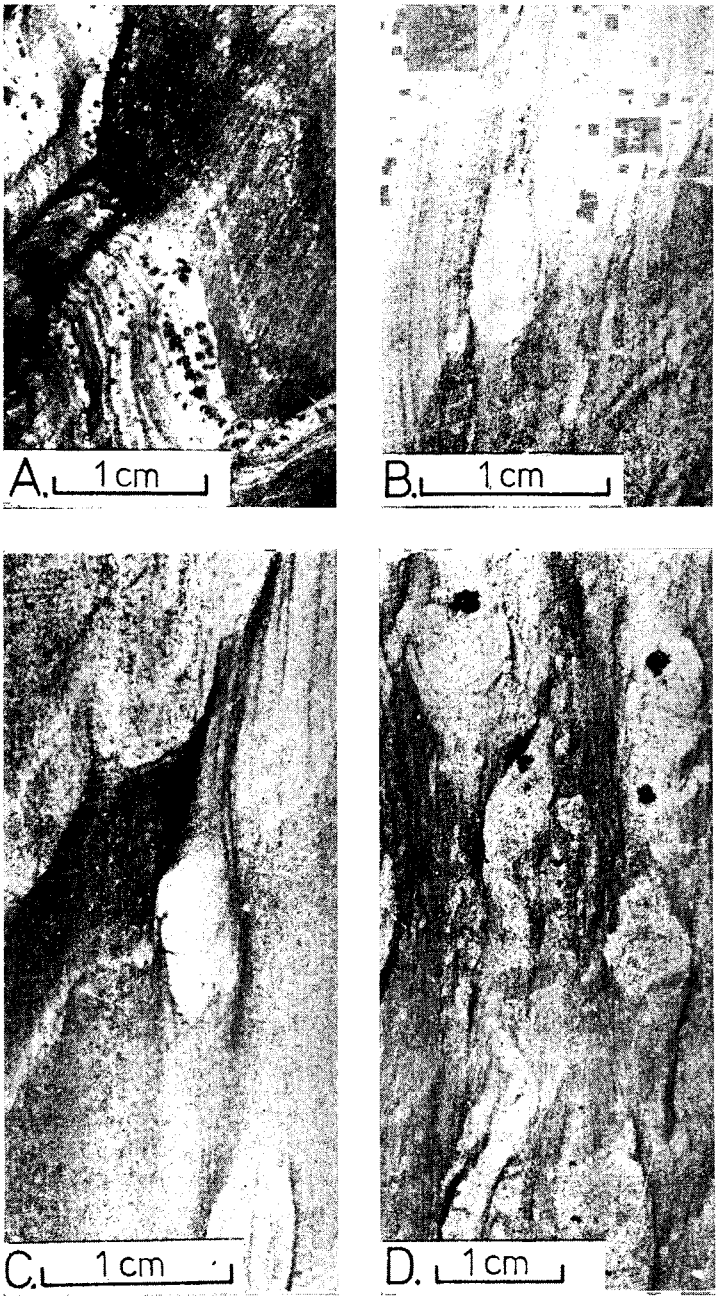


Group 2 mesoscopic structures. (A) $F_1$ mesoscopic fold deforming bedding ($S_0$) lamination; $S_1$ axial surface foliation trends in a northeast-southwest direction. (B) Mullion structure. $S_0$ trends northeast-southwest; $S_1$ trends north-south. (C) Isolated lobes of sandstone enclosed between $S_1$ surfaces; $S_0$ trends northeast-southwest. (D) More irregular lozenges of sandstone enclosed between $S_1$ surfaces.

PLATE 2

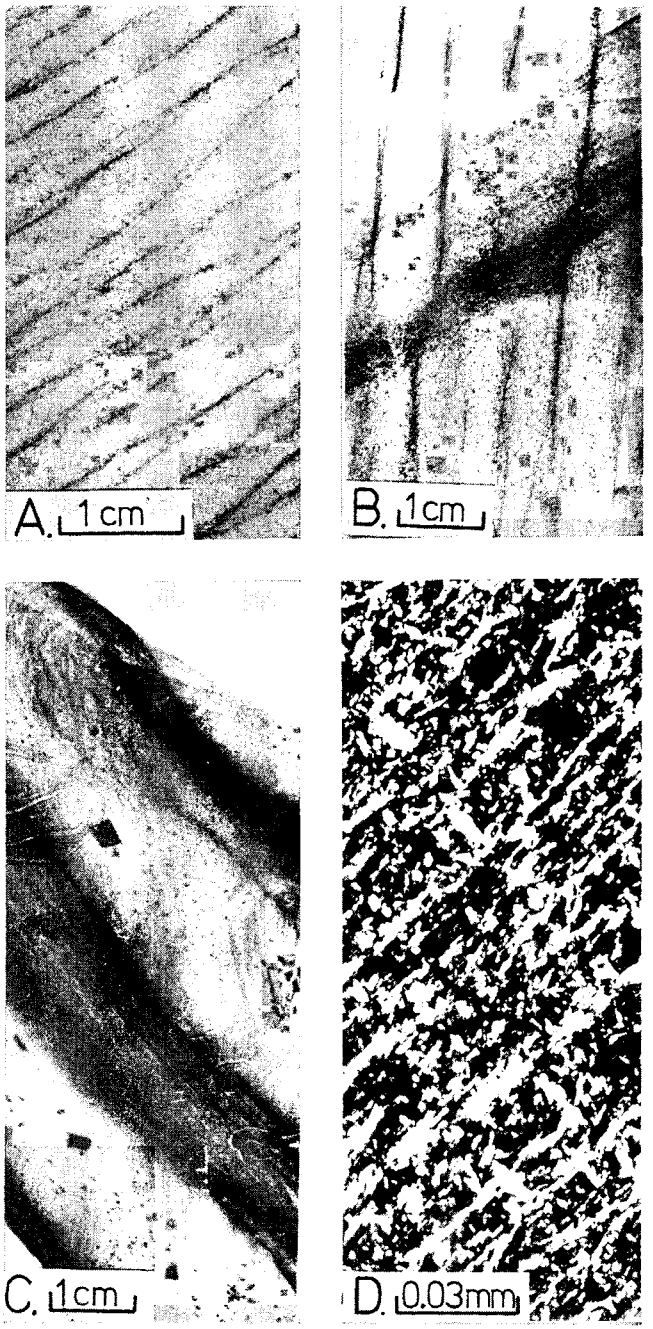


$S_1$ morphology. (A) Diffuse, anastomosing layering in homogeneous sandstone. (B) Variation of $S_1$ with lithology—anastomosing in sandstone (top and bottom of photograph); more widely spaced, planar and situated along the short limb zones of mesoscopic folds in bedding within the silty laminae. (C) Planar layering (northwest-southeast) along short limb zones of mesoscopic folds in cross-laminated $S_0$ (north-south) within laminated siltstone. (D) Crenulate structure in pelite; $S_1$ trends northeast-southwest, $S_0$ northwest-southeast.

MINERALOGY AND MICROSTRUCTURE

*Sandstones.*—The $S_1$ foliation in the sandstones is an irregular, anastomosing, metamorphic layering defined by relative concentrations of phyllosilicates (white mica + chlorite) and quartz, termed P-layers and Q-layers respectively. The P-layers are up to about 0.5 mm thick, are between 0 and 5 to 6 mm apart, and vary considerably in persistence (pl. 2-A). Folding is absent in the sandstones except within occasional interbedded coarse siltstone laminae which contain abundant white mica and chlorite; here the $S_1$ foliation changes gradually from the normal anastomosing type to a more widely spaced, planar type situated along the short limbs of mesoscopic folds in the siltstone laminae (pl. 2-B).

The Q-layers, within sections both parallel and perpendicular to $S_1$, are dominated by near-equant, detrital grains of quartz, generally 0.2 to 0.4 mm across, and albite clasts. Most quartz grains exhibit undulose extinction or deformation bands, while only a few contain deformation lamellae or subgrains; grain boundaries are either diffuse or have a corroded appearance, and the detrital grains are surrounded by a mass of small (<20 $\mu$m) grains. Albite clasts occur without overgrowths. The phyllosilicates within the Q-layers appear to belong to two distinct groups, distinguished on the basis of size, shape, orientation, and structure.

1. Coarse (0.05 to 0.4 mm long) white mica, chlorite, and interlayered white mica/chlorite (length:width ratios <10:1) are generally oriented oblique to the metamorphic layering and subparallel to bedding; such phyllosilicates occasionally exhibit undulose extinction or kinking, and several of the mica grains show pressure fringes (Spry, 1969) of quartz.

2. Fine-grained (30-60 $\mu$m long), needle-like white micas (length: width ratios generally >10:1) are oriented parallel to the gross metamorphic layering, cut across the bedding, and occur as single or composite grains spatially separate from the coarser micas; these mica grains characteristically exhibit no intracrystalline deformation features. Furthermore, such white mica partially to completely replaces chlorite within the thin, coarse siltstone laminae interbedded within the sandstones.

The P-layers contain the same minerals as the Q-layers, but there are significant differences in the modal amounts present, in the microstructure, and, as will be shown later, in the chemistry of the P-layers compared to the Q-layers. The following summarizes the compositional and microstructural differences.

1. The quartz and albite contents of the P-layers are reduced by a factor of 0.3 (table 1 and pl. 3-A).

2. The mica:chlorite ratio is 2:1 or higher in the P-layers compared to approx 1:1 in the Q-layers (table 1).

3. Detrital quartz grain size in the P-layers is reduced within sections both parallel and perpendicular to $S_1$ (pl. 3-A).

4. Detrital quartz grains display a more elliptical shape (major:minor axial ratio between 3 and 5:1 compared to between 1 and 2:1 in the Q-layers) and have a strongly corroded outline in the P-layers, grain long axes being parallel to the $S_1$ layering; this difference in quartz grain shape is particularly striking in sections perpendicular to $S_1$ (pl. 3-A).

5. The two groups of phyllosilicates described above can still be distinguished in the P-layers, but the more equidimensional phyllosilicates (group 1) are less well oriented parallel to $S_0$, and indeed several grains subparallel $S_1$. Furthermore, group 1 phyllosilicates in folded siltstone laminae interbedded within the sandstones (as, for example, the thin laminae in pl. 2-B) follow the $S_0$ trace around the fold and, thus, are rotated in limb areas subparallel to the $S_1$ orientation.

6. Group 1 phyllosilicates in the P-layers invariably show evidence for intracrystalline deformation including kinking and undulose extinction. Ti-rich oxide phases are often concentrated along the cleavages or irregular grain boundaries of the deformed phyllosilicates (pl. 3-B).

7. The P-layers are dominated by needle-like white mica (group 2 described above), oriented parallel to the metamorphic layering, and discontinuous trains of Ti-rich phases (pl. 3-C).

*Laminated siltstones.*—The $S_1$ foliation in the laminated siltstones is a planar and regular, differentiated crenulation cleavage (pl. 2-C). The P-layers vary from to 2.5 mm up to 1.5 cm thick and are usually $<2$ cm apart. The spacing of the P-layers is directly related to the shape of mesoscopic folds in siltstone laminae, the P-layers being concentrated along the limb nearer to the fold axial surface in asymmetric folds and along both limbs in symmetric folds.

Apart from the higher percentage of phyllosilicates in the siltstones (table 1), their mineralogy is similar to the sandstones. In particular, both groups of phyllosilicates can still be recognized and occur similarly to the sandstones; there is, however, abundant needle-like mica (group 2) in the Q- as well as the P-layers. As in the sandstones the P-layers are

TABLE 1

Modal analyses (determined by infrared analysis) of the major constituents of the P- and Q-layers within a sandstone and a laminated siltstone sample

| Mineral | Sandstone | | Laminated Siltstone | |
|---|---|---|---|---|
| | P-layers | Q-layers | P-layers | Q-layers |
| Quartz | 43±3 % | 65±3 % | 15±3 % | 54±3 % |
| Albite | 10±3 % | 15±3 % | 4±3 % | 8±3 % |
| Mica | ≃20 % | ≃7 % | ≃45 % | ≃18 % |
| Chlorite | ≃10 % | ≃5 % | ≃27 % | ≃13 % |

PLATE 3

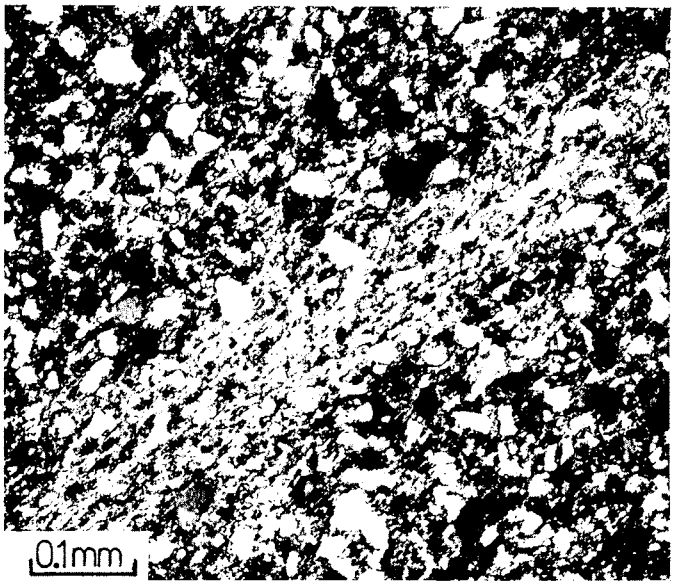


A. Contrast in composition, quartz grain size and grain shape between P- (trending northeast-southwest across the photograph) and adjacent Q-layers. Section perpendicular to the $S_1$ layering in a sandstone: Crossed nicols.

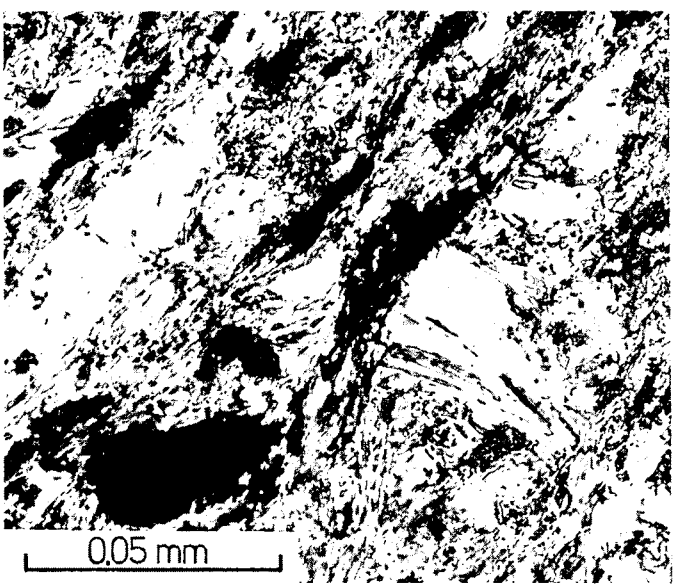


B. Ti-rich oxide phase (dark blebs) occurring within sandstone P-layer and concentrated particularly along the edge of deformed group 1 mica grain: Uncrossed nicols.

PLATE 3 (continued)

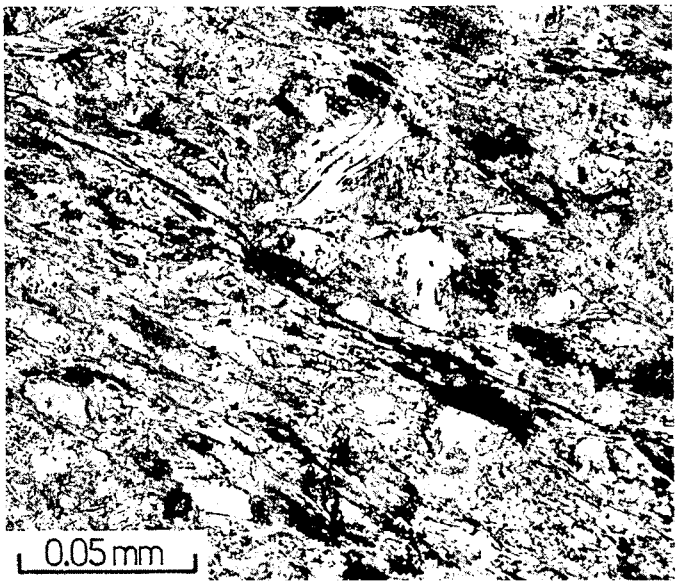


C. Detail of P-layer within sandstone showing deformed group 1 mica (northeast-southwest trend), needle-like group 2 micas oriented parallel to the layer (northwest-southeast) and discontinuous trains of Ti-rich oxide phase (dark blebs): Uncrossed nicols.

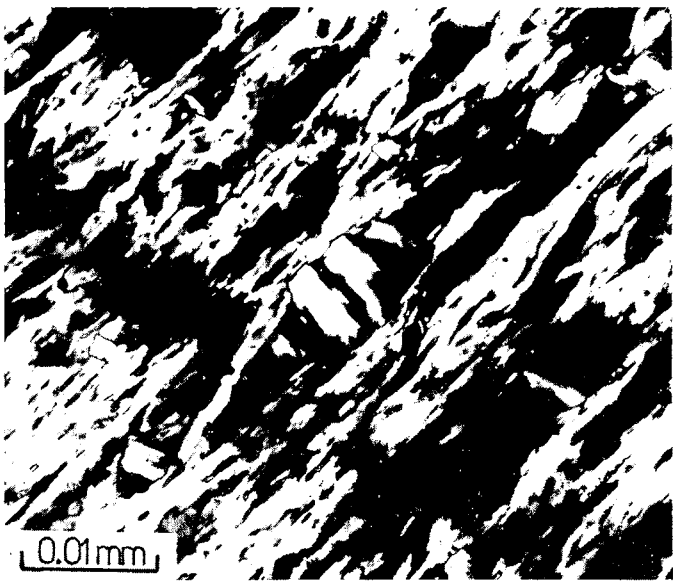


D. Domainal microstructure within laminated siltstone P-layer. Dark areas are chlorite flakes which together with the group 1 micas trend northwest-southeast; the group 2 micas trend northeast-southwest, parallel to the gross layering: Crossed nicols.

dominated by group 2 micas and discontinuous trains of Ti-rich minerals oriented parallel to the metamorphic layering. The distinctive features of the P- and Q-layers within the siltstones are now described.

1. The quartz content is reduced by a factor of about 0.5 to 0.75, and the albite content by a factor of 0.5 in the P-layers compared to the Q-layers within the siltstones (table 1).

2. Detrital quartz ranges from 10 to 40 $\mu$m in size, while the more equidimensional, group 1 phyllosilicates are about 50 $\times$ 10 $\mu$m.

3. Within the P-layers there is a characteristic domainal microstructure (pl. 3-D). The domains, which vary up to 0.1 mm long and 30 $\mu$m across in sections perpendicular to $S_1$, consist of group 1 phyllosilicates, often bent, but generally oriented oblique to the enclosing group 2 mica orientation which is parallel to $S_1$. Both the domain boundaries and the edges of the phyllosilicate grains within the domains are irregular; where group 1 mica and chlorite are interlayered within the domain, the boundary is recessed into the domain adjacent to the chlorite and protrudes into the enclosing group 2 needle-like mica adjacent to the group 1 mica (pl. 3-D).

4. Group 1 phyllosilicates commonly exhibit undulose extinction and kinking in both P- and Q-layers.

*Pelites.*—In hand specimen the $S_1$ foliation within the pelites has a slaty cleavage aspect. However, microscopic examination reveals well oriented but inhomogeneously distributed needle-like micas which are concentrated within discontinuous layers parallel to $S_1$ (pl. 2-D). On the coarsest scale, these layers are up to 0.1 mm thick and 0.3 mm apart. However, the microstructure of the pelites is dominated by mica layers, perhaps only 2 to 3 grains (up to 10 $\mu$m) thick, between which lie variably oriented and occasionally bent group 1 phyllosilicates (up to 30 $\times$ 10 $\mu$m) with highly irregular boundaries. Thus, the $S_1$ foliation in the pelites is a crenulation cleavage; the microstructure closely resembles that in the siltstone P-layers.

*Veins.*—Veins rich in quartz ($\pm$ chlorite) and sideritic carbonate are up to several millimeters thick and show a complex relationship to $S_1$. Several veins are discordant to $S_1$, while others are either parallel to $S_1$ or deformed by $F_1$ mesoscopic folds and strongly cleaved. In many quartz veins, the individual quartz grains show intracrystalline deformation, recovery and recrystallization characteristics; such features as undulose extinction, deformation bands, subgrains, and well formed new grains are far better developed in the vein quartz than in the detrital quartz of the host rock.

*Interpretation of microstructure.*—1. Group 1 mica is pre-$S_1$ and is considered to be detrital in origin, while group 2 mica is metamorphic and interpreted as syn-$S_1$.

2. Chlorite, which shows the same deformation features as the coarse group 1 micas, is also pre-$S_1$; there does not appear to be any metamorphic chlorite.

3. The better preservation of detrital grains in the Q-layers and the contrast in detrital quartz grain size and shape between the P- and Q-layers are inconsistent with differentiation models involving only addition of quartz and albite to or removal of phyllosilicates from the incipient Q-layers. Models involving more significant removal of quartz and albite from or addition of phyllosilicates to the incipient P-layers are, however, consistent with the data.

4. Since it appears to be difficult to leach Ti out of a rock and place it in solution (see discussion later), the presence of trains of Ti-rich oxide phases along the P-layers favors removal of more soluble material, such as quartz and albite, from the incipient P-layers with concomitant concentration there of less soluble material as the more important process. This interpretation is the same as the conclusions reached by Plessmann (1964), Williams (1972), and Gray (1977) for other such differentiated cleavages.

5. Highly irregular chlorite and detrital mica boundaries in the P-layers suggest that both these minerals are unstable there; the relationships within the domainal microstructure of the siltstone P-layers indicate, however, that chlorite is significantly less stable than mica. These points may well explain the higher mica:chlorite ratio in P- compared to Q-layers in both laminated siltstones and sandstones.

6. The occurrence of corroded quartz boundaries and the absence of overgrowths on particularly the albite clasts are inconsistent with significant transfer of material from the P- to the Q-layers; indeed, the grain boundary shapes suggest limited removal rather than addition of material in the Q-layers.

7. The oblique orientation and deformation of chlorite and detrital mica within the domainal microstructure of the siltstone P-layers suggest that the domains are relic hinges of microfolds in detrital phyllosilicates. The irregular domain boundaries are thought to correspond to the limb areas of these microfolds along which occurred marked diffusive activity with breakdown and removal of the components of chlorite and to a lesser extent detrital mica; the shape of these microfolds is also obscured by the concentration of well oriented group 2 mica on their limbs. The spatial independence of the metamorphic and detrital micas favors growth of the metamorphic mica parallel to $S_1$, rather than recrystallization of detrital mica.

8. The relationship between the quartz (± chlorite) and carbonate veins and $S_1$ is consistent with a continuously overlapping sequence of removal of material from the P- and to a less extent the Q-layers and precipitation of quartz (± chlorite) and sideritic carbonate in the veins.

9. It is suggested that dissolution reactions between trapped connate fluid and the various mineral species, on expulsion of this fluid during the $D_1$ deformation, could have effected the bulk transfer of material inferred from the microstructure of the different mineral species. In the pelites and laminated siltstones, the solution (and precipitation) activity

appears to have been most pronounced on the limbs of microscopic and mesoscopic folds; in the sandstones, solution (and precipitation) activity is still prominent even though folding is generally absent.

*Summary.*—The microstructural analysis establishes the complex nature of the $S_1$ foliation. It is not possible for any single mechanism to explain all the microstructural features. Intragranular deformation of quartz, breakdown and removal of quartz, albite, and phyllosilicates, and growth of new mica appear to have been particularly active during formation of $S_1$ in the sandstones. Folding of bedding laminae, rotation and deformation of detrital phyllosilicates within microfolds, breakdown and removal of quartz, albite, and phyllosilicates, and growth of new mica are all considered to have been significant processes in the formation of $S_1$ within the laminated siltstones and pelites. Interpretation of the microstructural data leads to a differentiation model involving preferential removal of material and new grain growth along certain, discrete zones. The situation of these zones is fold-dependent in the laminated siltstones and pelites, but, since folds are generally absent in the sandstones, such zones exist independent of folding in this lithology. These zones correspond to the dark P-layers. Removal of material out of the local system is favored over transfer from P- to Q-layers. This interpretation gains support when it is considered that the veins of quartz (± chlorite) and carbonate present within the Clunes metasediments provide a logical "sink" for the expelled material. In general, the microstructures testify to the importance of diffusive processes and new grain growth which both tend to obscure the effects of mechanical reorienting processes, particularly the rotation of detrital phyllosilicate grains within the laminated siltstones and pelites. Dissolution of material in trapped connate fluid is suggested to be the most likely material transfer mechanism acting during the protracted $D_1$ deformation.

## CHEMICAL AND VOLUME CHANGES DURING $S_1$ FORMATION

*Analytical procedure.*—P- and Q-layer material from 5 sandstone and 7 laminated siltstone samples were extracted using a small diamond wheel attached to a dental drill. Major and minor elements and the trace elements Y and Zr were analyzed using a Siemens single channel X-ray fluorescence spectrometer SRS-1. All elements, except Na, Y, and Zr which were analyzed using pressed powder pellets, were determined on lithium borate glass discs prepared from powdered samples, following the method described by Norrish and Hutton (1969). Y and Zr contents were calculated by comparison with U.S. Geological Survey Rock Standards. Individual whole rock analyses are available on request from either MBS or MJG.

*Results.*—Average chemical compositions of the P- and Q-layers within the 5 sandstone and 7 laminated siltstone samples are shown in table 2 (columns 1 to 4). Except for Si, Na, and possibly Mn, the P-layers are richer in all elements, and the enrichment factors (table 2, column 5) lie in the order K>Ti>Y>Zr>Al≅Mg>Fe≅P>Ca>Mn>Si>Na.

Except for K the enrichment factors are highest for the elements Ti, Y, Zr, Al, and, particularly in the laminated siltstones, the values for these four elements are consistent with one another. K is sited exclusively in white mica, most of which belongs to the group 2 metamorphic category. As will be shown later, these micas are cation deficient in the 12-fold coordination site; in particular, there are between 1.56 and 1.93 $K^+$ ions (avg = 1.76). It appears likely, then, that all the available K in the ambient pore fluid was fixed in the new micas, whether in the P- or the Q-layers, and that K did not leave the system during $S_1$ formation. Studies of the relative mobility of species show that Ti and Al, in particular, occur in very low concentrations in natural hydrothermal waters, indicating that leaching of these elements is exceptionally slow compared to other species, while K occurs in quite high concentrations (see,

TABLE 2

Average chemical analyses of the P- and Q-layers within 5 sandstone and 7 laminated siltstone samples

| | P-layers | | Q-layers | | Enrichment factor (P-layers) | No. of g. per g. $TiO_2$ | | No. of g. lost per g. $TiO_2$ | No. of g. lost per 100 g. rock | % Loss |
|---|---|---|---|---|---|---|---|---|---|---|
| | Mean | S.D. | Mean | S.D. | | P-layers | Q-layers | | | |
| | 1 | 2 | 3 | 4 | 5 | 6 | 7 | 8 | 9 | 10 |
| | | | | | Sandstones (5 analyses) | | | | | |
| $SiO_2$ | 62.87 | 0.72 | 76.56 | 1.68 | 0.82 | 69.86 | 174.60 | -104.14 | -48.82 | -60 |
| $TiO_2$ | 0.90 | 0.18 | 0.44 | 0.06 | 2.05 | 1.00 | 1.00 | - | - | - |
| $Al_2O_3$ | 17.52 | 0.95 | 10.88 | 1.13 | 1.61 | 19.47 | 24.73 | -5.26 | -2.31 | -21 |
| $Fe_2O_3^x$ | 5.17 | 0.73 | 3.54 | 0.44 | 1.46 | 5.74 | 8.05 | -2.31 | -1.02 | -29 |
| MnO | 0.04 | 0.04 | 0.04 | 0.03 | 1.00 | 0.04 | 0.09 | -0.05 | -0.02 | -50 |
| MgO(2) | 3.16 | 0.36 | 1.87 | 0.49 | 1.69 | 3.51 | 4.25 | -0.74 | -0.33 | -17 |
| CaO | 0.33 | 0.06 | 0.24 | 0.03 | 1.38 | 0.37 | 0.55 | -0.18 | -0.08 | -33 |
| $Na_2O$(3) | 1.20 | 0.17 | 1.88 | 0.40 | 0.64 | 1.33 | 4.27 | -2.94 | -1.29 | -69 |
| $K_2O$ | 4.43 | 0.53 | 2.02 | 0.43 | 2.19 | 4.92 | 4.59 | +0.33 | +0.15 | +7 |
| $P_2O_5$ | 0.23 | 0.05 | 0.15 | 0.02 | 1.53 | 0.26 | 0.34 | -0.08 | -0.04 | -27 |
| Loss | 5.50 | 0.40 | 3.34 | 0.52 | 1.65 | 6.11 | 7.59 | -1.48 | -0.65 | -20 |
| Total | 101.35 | | 100.96 | | | | | | | |
| Y (3) | 52 | 5 | 28 | 5 | 1.86 | 0.0058 | 0.0064 | -0.0006 | -0.0003 | -11 |
| Zr (3) | 254 | 65 | 150 | 21 | 1.69 | 0.0282 | 0.0341 | -0.0059 | -0.0026 | -17 |
| | | | | | Laminated Siltstones (7 analyses) | | | | | |
| $SiO_2$ | 51.50 | 2.67 | 69.40 | 3.42 | 0.74 | 53.65 | 130.94 | -77.29 | -40.96 | -59 |
| $TiO_2$ | 0.96 | 0.11 | 0.53 | 0.09 | 1.81 | 1.00 | 1.00 | - | - | - |
| $Al_2O_3$ | 22.65 | 1.05 | 13.52 | 1.83 | 1.68 | 23.52 | 25.51 | -1.92 | -1.01 | -8 |
| $Fe_2O_3^x$ | 8.28 | 0.93 | 6.00 | 0.92 | 1.38 | 8.62 | 11.32 | -2.70 | -1.43 | -24 |
| MnO | 0.06 | 0.04 | 0.08 | 0.07 | 0.75 | 0.06 | 0.15 | -0.09 | -0.05 | -63 |
| MgO | 3.94 | 3.59 | 2.49 | 0.36 | 1.58 | 4.10 | 4.70 | -0.60 | -0.32 | -13 |
| CaO | 0.22 | 0.04 | 0.22 | 0.03 | 1.00 | 0.23 | 0.42 | -0.19 | -0.10 | -46 |
| $Na_2O$ | 0.55 | 0.17 | 1.21 | 0.13 | 0.45 | 0.57 | 2.28 | -1.71 | -0.91 | -75 |
| $K_2O$ | 6.26 | 0.51 | 2.88 | 0.54 | 2.17 | 6.52 | 5.43 | +1.09 | +0.58 | +20 |
| $P_2O_5$ | 0.16 | 0.03 | 0.13 | 0.02 | 1.23 | 0.17 | 0.25 | -0.08 | -0.04 | -32 |
| Loss | 5.53 | 1.09 | 3.52 | 0.80 | 1.57 | 5.76 | 6.64 | -0.88 | -0.47 | -13 |
| Total | 100.11 | | 99.98 | | | | | | | |
| Y (6) | 59 | 8 | 35 | 3 | 1.69 | 0.0061 | 0.0066 | -0.0005 | -0.0003 | -9 |
| Zr (6) | 171 | 37 | 102 | 23 | 1.68 | 0.0178 | 0.0192 | -0.0014 | -0.0007 | -7 |

* Total Fe calculated as $Fe_2O_3$.
When number of values used to calculate average differs from that stated, the number used is shown in brackets next to the element concerned.
Major and minor elements in wt percent, Y and Zr in ppm.

for example, Helgeson, 1967). Studies of the behavior of the elements Ti, Y, and Zr during low-grade metamorphism of basaltic rocks (Cann, 1970; Pearce, 1975) confirms the relative immobility of Ti and shows that the trace elements Y and Zr are likewise stable. These considerations favor the interpretation that the significant concentration of the elements Ti, Y, Zr, and Al in the P-layers is due to their relatively low mobility, and they were enriched there due to the removal of other more mobile material, while the high enrichment factor for K is, indeed, due to a small addition of K to the P-layers during $S_1$ formation. Since Ti shows the highest enrichment factor of the elements Ti, Y, Zr, and Al, for the purpose of the following discussion it will be assumed that this element was completely conserved. Interpretation of the microstructure in the Q-layers does not favor significant transfer of the material lost from the P-layers to the adjacent Q-layers with concomitant volume increase there. The working hypothesis that the material lost from the P-layers has left the local system is, therefore, adopted.

The number of grams of each oxide per gram of $TiO_2$ in the P- and Q-layers is presented in columns 6 and 7 of table 2 respectively. On the basis that Ti neither left nor was added to the system and working with the hypothesis above, these figures "correct" the analyses of the P-layers to the values they would have assumed had there been no volume decrease due to removal of material. The difference between the values in these columns allows a quantitative estimate to be made of the loss of material during formation of the P-layers, relative to the composition of the Q-layers (table 2, columns 8, 9, and 10).

On a percentage basis and combining the figures for both lithologies, there appears to be highly significant ($\geqslant$40 percent) losses of Na, Si, Mn, and Ca, smaller (in the range 15 to 40 percent) yet significant losses of P, total Fe, volatiles, Mg, and Al, minor (<15 percent) losses of Zr and Y, and minor (<15 percent) addition of K during P-layer formation. Since the losses are calculated relative to the composition of the Q-layers where, as stated above, the microstructure also suggests some volume decrease during formation of $S_1$, the values are minimum estimates for the actual losses involved.

*Chemical changes in relation to mineralogy, microstructure, and lithology.*—The substantial loss of Na is consistent with a model involving greater dissolution of albite within the P-layers. Thus, in the sandstones, the calculated loss of Na is greater as more albite appears to have been available for dissolution. The highly significant loss of Si is consistent with the proposed dissolution of quartz in the P-layers; however, other phases (for example, albite, chlorite, white mica) may also have contributed considerable amounts of Si on breakdown. The loss of Fe and Mg, in particular, is compatible with dissolution of chlorite, although small amounts of Fe may have been supplied from the breakdown of sideritic carbonate, a reaction predicted from the substantial loss of Ca from the P-layers.

Al is not specific to any particular mineral; it would have been in abundant supply in a variety of original phases in the rock, including albite, chlorite, detrital mica, and, perhaps most important of all, matrix clay minerals. It can be calculated, however, that the observed loss of Al from the P-layers is less than the expected loss if the Al freed by the breakdown of albite and chlorite had all left the system. If detrital mica and matrix clays were also dissolving and potentially able to supply Al, then it is clear that Al largely remained in the rock and entered some new phase; the obvious place is the group 2 metamorphic micas which dominate the P-layers. Addition of K implies that this element was available in the pore fluid; the ready supply of Al in the rock allowed production of group 2 mica in considerable quantity. Minor loss of Al from the system and deficiency of $K^+$ ions in the 12-fold coordination site of the group 2 micas indicate that the availability of K in the pore fluid was the critical factor controlling the amount of group 2 mica actually produced.

*Summary and estimate of volume loss during $S_1$ formation.*—Consideration of the comparative bulk chemistry of the P- and Q-layers in the light of studies on the relative mobility of different species indicates that Ti (and to a lesser extent Y, Zr, and Al) was concentrated in the P-layers due to the removal of more mobile material (particularly Na, Si, Mn, and Ca), while a small amount of K was, indeed, added to the P-layers. On the basis that Ti was completely conserved and, as seems likely from the microstructural evidence, material migrated out of the local system rather than into adjacent Q-layers, estimates of the amount of K added and other elements lost (minimum values) during P-layer formation, relative to the composition of the Q-layers, have been made. This analysis predicts highly significant ($\geqslant$40 percent) losses of Na, Si, Mn, and Ca, smaller losses (15 to 40 percent) of P, total Fe, volatiles, Mg, and Al, minor losses ($<$15 percent) of Zr and Y, and minor ($<$15 percent) addition of K. Dissolution of albite, which exclusively sites the Na in the rock, and quartz, which mainly accounts for the Si, are consistent with the chemical data. Since K is sited exclusively in the white mica, which dominates the P-layers, it is inferred that a small amount of mica has also been added to the P-layers. Thus, the chemical data support the interpretation from the microstructural data that the $S_1$ layering formed mainly by removal of more mobile material, such as albite and quartz, from the incipient P-layers, while at the same time showing that a small amount of mica was also added to the incipient P-layers.

Since it is estimated that the P-layers occupy an average 10 to 20 percent of the rock volume, and the Ti values indicate a volume loss of about 50 percent during formation of a single P-layer, then the volume loss related to removal of soluble material during P-layer formation is in the order 10 to 20 percent of the original rock volume. This is a minimum estimate for the total loss in volume during $S_1$ formation, since there was probably some volume decrease due to removal of material from that part of the original rock that is now occupied by the Q-layers.

*Analytical procedure.*—Micas and chlorites were analyzed in carbon-coated thin sections with a Jeol JXA-5A electron microprobe using a slightly defocussed beam, where possible, to avoid volatilization of Na and K. Analyses of 69 micas and 18 chlorites are available from MBS on request. Analytical data are displayed in graphical form in figures 2 to 7; averages are listed in table 3.

*Mica chemistry.*—The compositions of the white micas have been recalculated in terms of three theoretical end-member components (H. W. Nesbitt, personal commun., 1975). The general formulae of these components are $Al_4Si_8O_{20}(OH)_4$ (pyrophyllite component), $X_{4-2}Al_4(Si_4Al_4)O_{20}(OH)_4$ (mica component), and $X_{2-1}(Y_{2-1}Al_2)Si_8O_{20}(OH)_4$ (phengite component), where X represents cations in the 12-fold coordination site (0 in the case of pyrophyllite; 4 monovalent or 2 divalent cations in the case of mica; 2 monovalent or 1 divalent cation in the case of phengite),

TABLE 3

Average chemical analyses of white micas and chlorites within P- and Q-layers

| | Group 1 Detrital Mica | | | | Group 2 Metamorphic Mica | | | | Chlorite | | | |
|---|---|---|---|---|---|---|---|---|---|---|---|---|
| | P-layers | | Q-layers | | P-layers | | Q-layers | | P-layers | | Q-layers | |
| | Mean (16) | S.D. | Mean (20) | S.D. | Mean (20) | S.D. | Mean (13) | S.D. | Mean (7) | S.D. | Mean (11) | S.D. |
| $SiO_2$ | 48.84 | 1.66 | 48.12 | 2.68 | 50.10 | 1.16 | 50.43 | 1.21 | 25.93 | 1.11 | 25.67 | 0.62 |
| $TiO_2$ | 0.38 | 0.17 | 0.40 | 0.24 | 0.36 | 0.17 | 0.34 | 0.18 | 0.11 | 0.10 | 0.18 | 0.30 |
| $Al_2O_3$ | 29.35 | 2.33 | 30.74 | 3.03 | 27.80 | 1.24 | 27.40 | 1.38 | 22.34 | 2.78 | 19.76 | 0.41 |
| FeO* | 2.63 | 0.61 | 2.42 | 0.92 | 3.25 | 0.63 | 3.14 | 0.81 | 25.78 | 2.14 | 27.35 | 0.92 |
| MnO | 0.02 | 0.02 | 0.02 | 0.02 | 0.02 | 0.02 | 0.02 | 0.01 | 0.17 | 0.07 | 0.26 | 0.04 |
| MgO | 2.13 | 0.77 | 1.63 | 0.89 | 2.64 | 0.33 | 2.24 | 0.36 | 12.09 | 0.79 | 12.78 | 0.43 |
| CaO | 0.00 | 0.00 | 0.00 | 0.00 | 0.00 | 0.00 | 0.00 | 0.00 | 0.00 | 0.00 | 0.00 | 0.00 |
| BaO | 0.17 | 0.08 | 0.16 | 0.05 | 0.12 | 0.02 | 0.07 | 0.05 | 0.00 | 0.00 | 0.00 | 0.00 |
| $Na_2O$ | 0.24 | 0.13 | 0.38 | 0.21 | 0.11 | 0.07 | 0.26 | 0.21 | 0.01 | 0.02 | 0.03 | 0.03 |
| $K_2O$ | 10.41 | 0.53 | 10.33 | 0.43 | 9.94 | 0.48 | 9.84 | 0.43 | 0.28 | 0.22 | 0.06 | 0.04 |
| Total | 94.17 | | 94.20 | | 94.34 | | 93.74 | | 86.71 | | 86.09 | |
| Ions per formula unit calculated on the basis of 22(0) for micas and 28(0) for chlorites | | | | | | | | | | | | |
| Si | 6.61 | 8.00 | 6.51 | 8.00 | 6.76 | 8.00 | 6.83 | 8.00 | 5.52 | 8.00 | 5.58 | 8.00 |
| $Al_{TET}$ | 1.39 | | 1.49 | | 1.24 | | 1.17 | | 2.48 | | 2.42 | |
| $Al_{OCT}$ | 3.29 | 4.06 | 3.41 | 4.05 | 3.18 | 4.12 | 3.21 | 4.06 | 3.13 | 11.70 | 2.64 | 11.86 |
| Ti | 0.04 | | 0.04 | | 0.04 | | 0.04 | | 0.02 | | 0.03 | |
| Fe* | 0.30 | | 0.27 | | 0.37 | | 0.36 | | 4.59 | | 4.97 | |
| Mn | - | | - | | - | | - | | 0.03 | | 0.05 | |
| Mg | 0.43 | | 0.33 | | 0.53 | | 0.45 | | 3.84 | | 4.14 | |
| Ca | - | 1.87 | - | 1.89 | - | 1.75 | - | 1.77 | - | | - | |
| Ba | 0.01 | | 0.01 | | 0.01 | | - | | - | | - | |
| Na | 0.06 | | 0.10 | | 0.03 | | 0.07 | | 0.01 | | 0.01 | |
| K | 1.80 | | 1.78 | | 1.71 | | 1.70 | | 0.06 | | 0.02 | |

* Total Fe calculated as FeO($Fe^{2+}$).
All elements in wt percent.
Number of analyses shown in brackets at head of each column of analyses.

and Y represents cations substituting in two octahedral sites (2 divalent or 1 tetravalent). The particular situation of interest here is where X = $K^+$, Y = $Fe^{2+}$, $Mg^{2+}$, $Mn^{2+}$, or $Ti^{4+}$, and only Al–Si substitution occurs in the tetrahedral site. The composition fields of various common white micas in this system are illustrated in the ternary plot (fig. 2, left triangle). The average compositions of the group 1 (detrital) and group 2 (metamorphic) micas in both P- and Q-layers are given in table 3.

A plot of all the Clunes micas on the ternary diagram (fig. 2, right triangle) shows a large spread within the phengite field, indicating dominant cation substitution in the octahedral and tetrahedral sites. This characteristic allows the mica chemistry variation to be expressed succinctly in terms of the mole percentage of phengite component (abbreviated to phengite component here).

A frequency distribution diagram (fig. 3A), employing this parameter separately for the detrital and metamorphic micas, indicates the wider range in chemical composition of the former and the tendency for the latter to lie at the more phengitic extreme of the detrital mica range; these characters are also illustrated in the standard ternary plot (fig. 3B). Whereas group 1 micas spread in composition from below 15 to 50 percent phengite component, group 2 micas lie in the range 32 to 51 percent with two thirds lying between 35 and 45 percent phengite component. On the present data, the two groups of micas are chemically

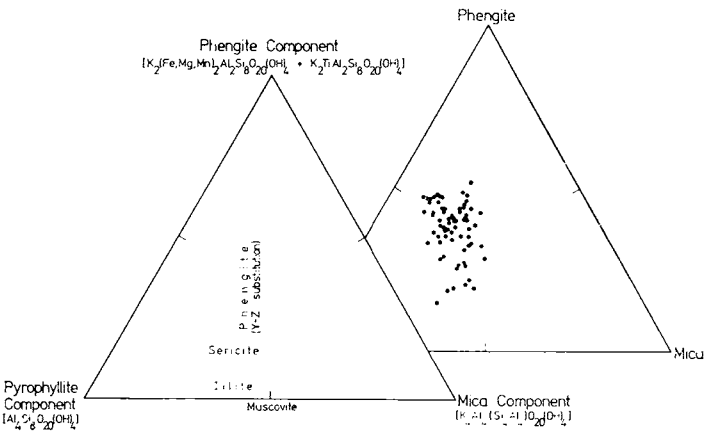


Fig. 2. Left triangle—chemical variation in white micas, where K occupies the 12-fold coordination site, Fe–Mg–Mn–Ti substitution occurs in the octahedral site, and Al–Si substitution occurs in the tetrahedral site. Chemistry expressed in terms of 3 end-member components (H. W. Nesbitt, personal commun., 1975).

Right triangle—variation in chemical composition of white mica from Clunes. Phengite component is calculated first by allotting all Fe–Mg–Mn–Ti to this component and balancing (K+Na), Al, and Si accordingly. Mica component is calculated second by allotting all remaining (K+Na) to this component and balancing Al and Si accordingly. Pyrophyllite component is calculated last by allotting remaining Al (or Si) to this component and balancing Si (or Al) accordingly.

distinct below the 30 percent phengite component level. These facts support the separation of the different micas on structural criteria.

The tendency for group 1 and 2 mica compositions to converge may be explained in two ways.

1. The detrital micas vary intrinsically in composition, and convergence toward the metamorphic mica composition range is coincidental.

2. The pre-metamorphic composition of the detrital micas was fairly uniform and close to muscovite, but during metamorphism they attempted to equilibrate with the ambient pore fluid and thus approached, with a variable degree of success, the more phengitic composition of the metamorphic micas; this involved substitution without destroying the muscovite structure of $Fe^{2+}$, $Mg^{2+}$, and $Si^{4+}$ for $Al^{3+}$.

Figure 4 shows there is a wide range in the $TiO_2$ content of the detrital micas that are low in the $K_2(Fe,Mg,Mn)_2Al_2Si_8O_{20}(OH)_4$ component. However, as this component increases, there is convergence of the $TiO_2$ content of the micas to low values. This can be explained by invoking some initial variation in $TiO_2$ content within the detrital micas which, during deformation and metamorphism, tends to be eradicated as the $Ti^{4+}$ migrates out of the $TiO_2$-rich micas and enters some new boundary phase. Two possible mica alteration paths are indicated sche-

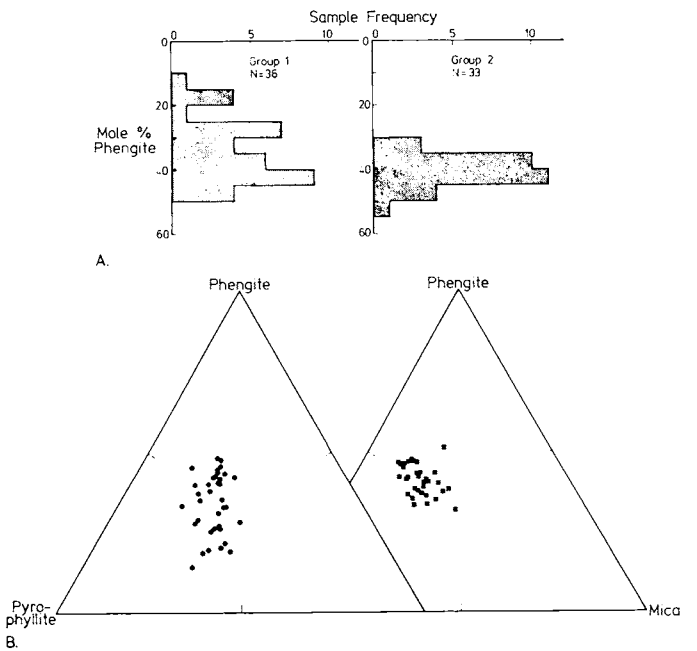


Fig. 3. (A) Composition (mole percent phengite) distributions of group 1 and group 2 micas.

(B) Composition of group 1 (left triangle, dots) and group 2 (right triangle, squares) micas.

matically in figure 4; paths 1 and 2 apply to detrital micas with initially high and low $TiO_2$ contents respectively. This explanation is consistent with the observation that Ti-rich oxide phases are often concentrated along the cleavages or at the edges of detrital micas, and often such Ti-rich trains help to define the $S_1$ cleavage. Thus, the detrital micas do appear to have changed composition during deformation and metamorphism suggesting that the second hypothesis above is the more reasonable, and the group 1 micas were initially close to muscovite in composition.

Whereas the metamorphic mica average composition (42 percent compared with 40 percent phengite component) and composition range (33 to 48 percent compared with 32 to 51 percent phengite component) are similar in the P- and Q-layers respectively (fig. 5), the detrital micas show certain differences in composition between the metamorphic layers (fig. 6). In the P-layers only 3 of the 16 micas analyzed have less than 30 percent phengite component, and 50 percent of the analyses are in the 40 to 45 percent range. The Q-layer detrital mica compositions are, however, more evenly dispersed over the total range in mica compositions, with 50 percent of the analyses falling below the 30 percent level. Since the metamorphic micas show similar compositions in the P- and Q-layers, it can be inferred that the composition of the fluid from which they precipitated was of similar composition in both layers. Thus, it is concluded that, although it was thermodynamically feasible for the detrital muscovites to reach equilibrium with an ambient fluid of similar composition in both layers, complete equilibrium has not been attained in either

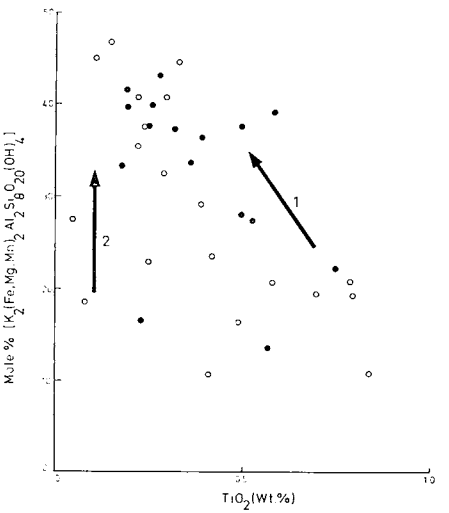


Fig. 4. Change in $TiO_2$ content of group 1 micas in both P- (dots) and Q- (open circles) layers with increasing content of the component $K_2(Fe,Mg,Mn)_2Al_2Si_8O_{20}(OH)_4$; possible mica alteration paths are indicated by the arrows—for explanation see text.

layer but appears more advanced in the P- compared to the Q-layers. In other words, the rate of the chemical reaction

$$\text{muscovite} + 0\text{–}2(\text{Fe,Mg})^{2+} + 0\text{–}2\text{Si}^{4+} \rightarrow \text{phengite} + 0\text{–}4\ \text{Al}^{3+}$$

is promoted in the P- compared to the Q-layers, such that in the P-layers the composition of the detrital micas more closely approximates that of the metamorphic micas.

Two important stages involved in the reaction are:

1. migration of ionic species through the detrital muscovite lattice;
2. migration of ionic species toward and away from the detrital muscovite lattice.

Any processes that promote ionic transfer during these stages would clearly assist the reaction cited above. Both stages are now considered in more detail. The analysis that follows employs Fick's 1st and 2nd laws of diffusion for the steady-state (concentration gradient constant) and non-steady-state (concentration gradient not constant) situations respectively;

$$\frac{\partial m}{\partial t} = -D\,\frac{\partial c}{\partial x}$$

and

$$\frac{\partial c}{\partial t} = D\,\frac{\partial^2 c}{\partial x^2}$$

where m is a quantity of matter transferred through unit cross section in unit time, c is concentration, t is time, x is distance, and D is the diffusion coefficient.

If the diffusion of a particular ion through a detrital muscovite is considered in both P- and Q-layer situations, it is apparent from the equations above that, whether a steady-state or non-steady-state condition is assumed, the variables determining the concentration of that

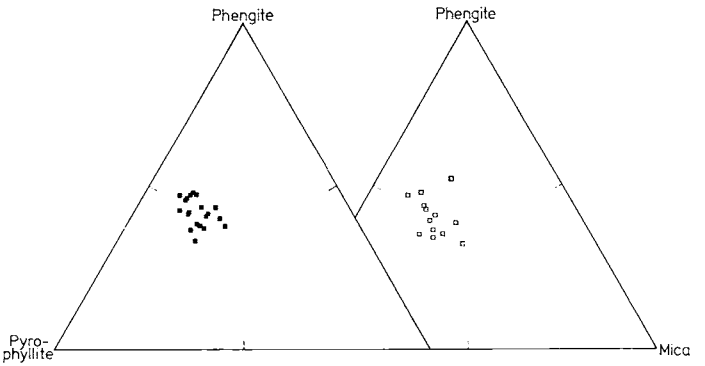


Fig. 5. Composition of group 2 micas in P-layers (left triangle, full squares) and Q-layers (right triangle, open squares).

ionic species at any comparable reference point in the two micas (for example the center of the grain) are:

1. the concentration of the ionic species on the edge of the muscovite, that is, the concentration of the species in the ambient pore fluid;
2. the size of the muscovite, that is, the distance over which diffusion has operated;
3. the time over which the diffusion process has operated;
4. the value of the diffusion coefficient, that is, the diffusivity of the particular muscovite grain.

It has already been inferred that the pore fluid had approximately the same composition in the two layers. Furthermore, the size of the detrital muscovites and the time over which diffusion has operated are similar in both layers. Thus, as far as intra-muscovite diffusion is concerned, only a higher diffusion coefficient in the P-layer detrital muscovites would promote the chemical reaction, cited above, in the P- compared to the Q-layers.

In this regard, it is recalled that the P-layer detrital muscovites are conspicuously more deformed than their counterparts in the Q-layers. An increase in ionic diffusivity related to zones of increased intra-crystal-

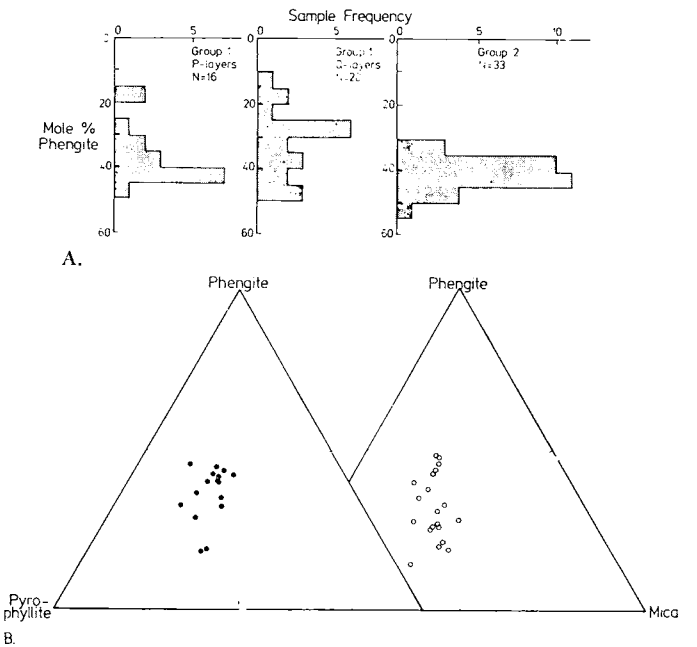


Fig. 6. (A) Composition (mole percent phengite) distributions of group 1 micas in P- and Q-layers. The composition distribution of all 33 group 2 micas is included for reference.

(B) Composition of group 1 micas in P-layers (left triangle, dots) and Q-layers (right triangle, open circles).

line deformation has been described by White (1975) for naturally deformed and partially recrystallized oligoclase, and this phenomenon is also known in metals (Cohen, 1970). Thus, it is suggested that increased diffusivity within the detrital muscovites of the P-layers is attributable to their more deformed character.

On the basis that Ti was completely conserved and concentrated in the P-layers due to more significant removal of mobile material from these layers, it can be shown that more fluid passed through the P- compared to the Q-layers. Enhanced fluid flow along the P-layers would favor easier transfer of ionic species toward and away from P-layer detrital muscovites. Furthermore, the volume loss implicit in P-layer formation would effectively decrease the distance over which ions would have to be transferred before encountering an unaltered muscovite grain. Both these factors would promote the reaction cited above in the P- compared to the Q- layers.

The above arguments suggest that ionic transfer both wthin and between detrital muscovite grains is promoted in the P- compared to the Q-layers.

*Chlorite chemistry.*—The $Si^{4+}$ necessary for the conversion of muscovite to phengite would have been readily available in the pore fluid due to dissolution of various detrital silicates, in particular quartz. However, the source for the $Fe^{2+}$ and particularly the $Mg^{2+}$ would have been the chlorite.

Microstructural considerations suggest the dissolution of some chlorite, particularly in the P-layers. The arguments below also imply significant changes in the composition of the P-layer chlorites, chemical changes that lead, in particular, to the release of $Fe^{2+}$ and $Mg^{2+}$.

Figure 7 summarizes the compositional variation in the chlorites using the parameters $Al_{TET}/Si$ and $Al_{OCT}/Fe+Mg$ to specify individual chlorite compositions (average chlorite compositions from both P- and Q-layers are shown in table 3). Whereas the Q-layer chlorites are rela-

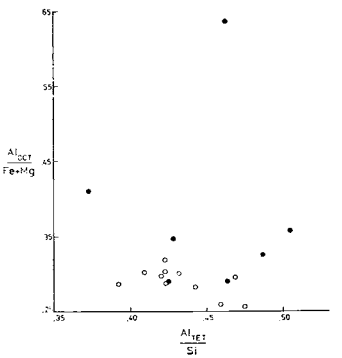


Fig. 7. Variation in composition of the pre-$S_1$ chlorites. P-layer chlorites are represented by a dot, Q-layer chlorites by an open circle.

tively well clustered, the P-layer chlorites are widely dispersed and are identified by higher $Al_{OCT}/Fe+Mg$ values and more extreme $Al_{TET}/Si$ values. The fact that the chlorite chemistry is different in the P- and Q-layers suggests that chemical changes induced during deformation and metamorphism are responsible rather than variation in the pre-metamorphic composition of the chlorites.

The larger compositional field of the P-layer chlorites is interpreted in terms of their greater "alteration" compared to the Q-layer chlorites. The marked tendency toward higher $Al_{OCT}/Fe+Mg$ values is consistent with diffusion of $Fe^{2+}$ and $Mg^{2+}$ out of the chlorite lattice.

Besides dissolution and ion exchange reactions, a few chlorites are partially to completely pseudomorphed by small metamorphic phengites (group 2 micas). Such replacement has only been noted in thin siltstone laminae interbedded in the sandstones. A reaction similar to that given below is envisaged:

$$4\underset{\text{chlorite}}{Mg_4Fe_5Si_6Al_5O_{20}(OH)_{16}} + 11Si^{4+} + 8.5K^{+} + 4H^{+}$$

$$\rightarrow 5\underset{\text{phengite}}{K_{1.7}Mg_{0.5}Fe_{0.5}Si_7Al_4O_{20}(OH)_4} + 13.5Mg^{2+} + 17.5Fe^{2+} + 24H_2O$$

The chlorite composition quoted here is the average of the Q-layer chlorites shown in figure 7, the phengite composition is the average metamorphic mica composition (see table 3), and the equation has been balanced assuming static $Al^{3+}$. The ionic charges on each side of the equation do not exactly balance, as the chlorite and phengite compositions employed are not ideal.

*Summary.*—Ion exchange reactions between pre-$S_1$ phyllosilicates and the ambient pore fluid during $D_1$ deformation and metamorphism explain the chemical heterogeneities of the detrital muscovites and pre-$S_1$ chlorites. By the substitution of $Fe^{2+}$, $Mg^{2+}$, and $Si^{4+}$ for $Al^{3+}$, muscovite tends toward the metamorphic phengite composition; loss of $Fe^{2+}$ and $Mg^{2+}$ and enrichment in $Al^{3+}$ are apparent in the chlorites. Complete chemical equilibrium between the detrital muscovites and the ambient pore fluid, which had approximately the same composition in both P- and Q-layers, has certainly not been achieved. However, the equilibrium situation is more advanced in the P- compared to the Q-layers. Considerations relating to why the rate of such chemical reactions are promoted in the P-layers are far more important than unqualified thermodynamic arguments.

Increased diffusivity of ionic species within detrital muscovite as well as easier migration of ionic species toward and away from such grains are both favored in the P- compared to the Q-layers. It is suggested that the more deformed nature of the P-layer detrital muscovites is the factor controlling more rapid intra-muscovite diffusion. Enhanced fluid flow along the P-layers and the volume loss implicit in their for-

mation are the favorable circumstances leading to easier transfer of ionic species toward and away from P-layer detrital muscovites.

## DISCUSSION

A model for the development of the $S_1$ foliation in the Clunes metasediments, consistent with the structural interpretation and the conclusions from the whole rock and phyllosilicate chemical data, is given below. It is suggested that the foliation formed by a complex interaction of mechanical and chemical factors.

Within the sandstones the strain was largely taken up by intra-crystalline deformation of individual quartz grains and the flattening and linking of preexisting pores giving rise to increased permeability. Since folding is absent, the linking pattern of deformed pores will be related to the sandstone packing characteristics prior to initiation of the $D_1$ strain. In the more anisotropic laminated siltstones and pelites the $D_1$ strain gave rise to folding of bedding laminae, rotation and bending of detrital phyllosilicates, as well as flattening and linking of pores. Reorientation of quartz-phyllosilicate grain boundaries and pore shape changes both assisted in increasing the permeability of these rocks, particularly along the limb zones (high strain areas?) of folds in bedding and pre-$S_1$ phyllosilicate microfolds; in asymmetric structures the effect was largely confined to the limb nearer to the fold axial surface, while in symmetric structures both limbs appear to have been susceptible to permeability enhancement. The net result is a diffuse, rather closely spaced pattern of high permeability zones in the sandstones and a more regular system of planar zones in the laminated siltstones and pelites, the spacing between which is determined by the half wavelength of the mesoscopic and microscopic folds. Such zones provide the most convenient path for any connate fluid trapped in the sediments—particularly the pelites—to escape and in this sense they are equivalent to the "channel-ways" of Williams (1972). The P- and Q- layers correspond to the zones of relatively high and low permeability respectively, and, thus, the contrast in $S_1$ morphology between the sandstones, laminated siltstones, and pelites is ultimately related to original differences in anisotropy between the different lithologies.

Chemical interaction between sediment and pore fluid expelled during the $D_1$ deformation occurred throughout all the rocks, but the effects of the chemical reactions are far more pronounced along the relatively high permeability zones; in particular, the *rate* of ion exchange reactions is promoted along such zones due both to increased diffusivity of ionic species within and between pre-$S_1$ mineral grains. Specific chemical reactions include:

1. dissolution of detrital quartz, albite, and probably pre-$S_1$ white mica, early diagenetic sideritic carbonate and pre-$S_1$ chlorite of uncertain origin;

2. ion exchange between the pore fluid and the pre-$S_1$ phyllosilicates leading to the in situ conversion of muscovite to phengite and the development of Al-rich chlorites;

3. occasional replacement of chlorite by fine-grained phengitic mica;

4. precipitation and growth of new phengitic mica in a strong preferred orientation parallel to the metamorphic layering.

Provision of cations to the ambient pore fluid via the dissolution reactions (1) leads to the ion exchange and replacement reactions (2 and 3) as the remaining pre-$S_1$ phyllosilicates attempt to attain equilibrium with the pore fluid. The principal reaction is the removal from the fluid of Si, K, and to a less extent Fe and Mg and combination with Al readily available in the rock to form the new metamorphic micas with phengitic composition (reaction 4). However, highly significant quantities ($\geqslant$40 percent) of Na, Si, Mn, and Ca, smaller amounts (15 to 40 percent) of P, total Fe, volatiles, Mg, and Al, and minor ($<$15 percent) amounts of Zr and Y appear to have been lost from and a minor ($<$15 percent) amount of K appears to have been added to the system during formation of the P-layers. A minimum estimate for the total loss in volume during $S_1$ formation lies in the range 10 to 20 percent of the original rock volume. Thus, although the differentiation of the Clunes sediments into P- and Q-layers is initially related to the establishment of relatively high and low permeability zones, the present character of the layers is determined by the more pronounced chemical changes that occurred along the high permeability zones.

It is suggested that the preferred orientation of the metamorphic micas resulted from an orientation-dependent growth mechanism, involving both the anisotropic supply of constituent material to the faces of newly precipitated mica grains and the anisotropic growth rate of mica crystals (Etheridge, Paterson, and Hobbs, 1974). This mechanism is favored, since, by definition, it incorporates the permeability of the system following the onset of strain as a vital consideration.

Material transported out of the local system is thought to have been precipitated largely in the quartz ($\pm$ chlorite) and carbonate veins which transect the Clunes metasediments. The complex relations between such veins, the $S_1$ layering and the $F_1$ mesoscopic folds, indicate that there is no straightforward time sequence in the operation of the various processes discussed above. After some initial strain increment, fluid migration, dissolution and precipitation of material, ion exchange reactions, and vein formation proceeded synchronously with subsequent strain increments.

The following considerations are of fundamental significance in the foliation model.

1. The dark P-layers, with their varied morphology in different lithologies, correspond to zones of relatively high permeability established during the $D_1$ deformation. The situation of the P-layers is fold-dependent in the laminated siltstones and pelites, but they exist even though folding is absent in the sandstones.

2. Substantial loss of material from the P-layers, particularly silica due to the dissolution of quartz, as well as minor addition of mica to the P-layers are both required. Interpretation of the Q-layer microstructure

suggests that there was no significant transfer of the material lost from the P-layers to the adjacent Q-layers; it appears instead that this material largely moved out of the system via the high permeability zones, leading to a net loss in volume during formation of $S_1$.

3. The same ion exchange reactions in phyllosilicates occurred in both P- and Q-layers, but the rate of such reactions was substantially faster along the P-layers.

Thermodynamic considerations (see review by Paterson, 1973) predict migration of material along chemical potential gradients established in response to gradients in applied stress. Such considerations are fundamental to the concept of pressure solution, defined by Voll (1960) as differential solution and redeposition in a stressed aggregate. Furthermore, several authors, including Plessmann (1964), Durney (1972), Williams (1972), Groshong (1975), and Cosgrove (1976), have discussed the role of pressure solution in the formation of cleavage surfaces. Stress gradients undoubtedly would have existed between the limb and hinge zones of developing folds in the laminated siltstones and pelites of the present study. Variation in the mean principal stress at grain contacts within such folds may well have been an important factor in determining sites of preferentially high solution in the laminated siltstones and pelites. However, the irregular, anastomosing nature of the $S_1$ foliation in the more homogeneous sandstones requires, applying the same model, that the mean principal stress at grain contacts shows considerable and highly localized, irregular fluctuations. The question arises whether the variations in mean principal stress at grain contacts are sufficiently high and sufficiently local in scale to explain the highly significant mineralogical and chemical differences between the P- and Q-layers.

It has been demonstrated in the Clunes sediments that the rate of ion exchange reactions was faster along the P-layers, and it is considered that enhanced fluid flow along such layers was an important factor contributing to the rate increase. It is suggested that the dissolution and mica precipitation reactions, which like the ion exchange reactions occurred in both P- and Q-layers, also proceeded at an increased rate in the P-layers due to the greater passage of fluid along these layers. In this model differentiation of the Clunes sediments into dark P- and light Q-layers is thought to be related to an increase in the rate of dissolution and mica precipitation reactions along high permeability zones, the incipient P-layers. Such a model, being intrinsically dependent on permeability factors, is applicable equally well to the formation of P-layers in both the sandstones and the more anisotropic laminated siltstones and pelites. However, there is nothing in this model that precludes that pressure solution effects are occurring at the same time.

## SUMMARY

1. The $S_1$ foliation, a metamorphic layering in the sandstones and a differentiated crenulation cleavage in the laminated siltstones and

pelites, formed by a complex interaction of mechanical and chemical processes.

2. Intragranular deformation of quartz, pore shape changes, and solution-mica precipitation reactions, particularly along preferential zones, are thought to have been significant processes in the formation of $S_1$ in the sandstones.

3. Folding of bedding laminae, rotation and deformation of pre-$S_1$ phyllosilicates, pore shape changes and solution-mica precipitation reactions, particularly along meso- and microfold limb zones, appear to have been important in the formation of $S_1$ in the laminated siltstones and pelites.

4. The domainal microstructure, conspicuous in the siltstone P-layers, is interpreted as relic hinges of microfolds in pre-$S_1$ phyllosilicates. The microfold shape is obscured due to dissolution and removal of, particularly, chlorite, and the growth of new, fine-grained mica along the microfold limbs.

5. The zones along which solution-mica precipitation reactions were prominent are considered to correspond to zones of relatively high permeability established during the early stages of the $D_1$ deformation. It is suggested that dissolution of material occurred in trapped connate fluid as it was expelled along the high permeability zones during the protracted $D_1$ deformation. Such high permeability zones are represented now by the dark, phyllosilicate- and Ti-rich P-layers; the light, quartz-rich zones, where solution-mica precipitation reactions were not as prominent, correspond to the Q-layers.

6. Ti and to a lesser extent Y and Zr (and Al) appear to have been concentrated in the P-layers due to the removal of more mobile material during formation of the metamorphic layering. Highly significant ($\geqslant$40 percent related to the composition of the Q-layers) losses of Na, Si, Mn, and Ca and smaller (15 to 40 percent related to the composition of the Q-layers) losses of P, total Fe, volatiles, Mg, and Al are indicated during formation of the metamorphic layering. Breakdown and dissolution of albite, quartz, pre-$S_1$ chlorite, diagenetic carbonate, and probably also pre-$S_1$ white mica are consistent with this data.

7. A small amount ($<$15 percent related to the composition of the Q-layers) of K appears to have been added to the P-layers during formation of the metamorphic layering. Since K is sited exclusively in the white mica, which dominates the P-layers, it is apparent that there was a small addition of mica to the P-layers. Availability of Al in the rock (matrix clay minerals, detrital mica, et cetera) and K in the pore fluid allowed production of group 2 metamorphic mica in considerable quantity. Since a small loss of Al did occur and the group 2 micas show deficiency of $K^+$ ions in the 12-fold coordination site, it is inferred that the availability of K in the pore fluid was the critical factor controlling the amount of group 2 mica actually produced.

8. Material lost from the P-layers is thought to have been transported out of the local system and to have been deposited in quartz (± chlorite) and carbonate veins which transect the Clunes metasediments. A minimum estimate for the total loss in volume during $S_1$ formation is 10 to 20 percent.

9. The new group 2 micas, at equilibrium with the ambient pore fluid, are similar in composition in both P- and Q-layers, suggesting that the composition of the fluid was the same in both layers. The new micas are conspicuously phengitic, that is, richer in Si, Fe, and Mg compared to the detrital micas. It is suggested that the preferred orientation of the new micas resulted from an orientation-dependent growth mechanism, involving both the anisotropic supply of material to newly precipitated grains and the anisotropic growth rate of mica (Etheridge, Paterson, and Hobbs, 1974).

10. Remaining detrital muscovite and pre-$S_1$ chlorite attempted to equilibrate with the ambient pore fluid via ion exchange reactions. Detrital muscovite approached the phengite composition by the substitution of $Fe^{2+}$, $Mg^{2+}$, and $Si^{4+}$ for $Al^{3+}$, and $Al^{3+}$ replaced $Fe^{2+}$ and $Mg^{2+}$ in the chlorites. $Ti^{4+}$ appears to have migrated out of detrital, $TiO_2$-rich muscovites and entered a new phase (hydrated oxide?) along the cleavages or at the edges of detrital muscovite grains. Occasional chlorite is also pseudomorphed by fine-grained phengite.

11. The rate of such ion exchange reactions was substantially faster along the P-layers, leading to a more advanced equilibrium situation in the P- compared to the Q-layers. The more deformed nature of the P-layer detrital muscovites promoted more rapid intra-muscovite diffusion, while increased fluid flow and volume reduction along the P-layers effected easier transfer of ions toward and away from P-layer detrital muscovite sites.

12. It is considered that the extreme mineralogical and chemical differences between adjacent P- and Q-layers as well as the highly variable $S_1$ morphology in different lithologies raise the question of whether the mechanism of pressure solution is solely responsible for the greater dissolution and precipitation of material along the incipient P-layers. It is suggested that dissolution and mica precipitation reactions occurred in both P- and Q-layers but, like the ion exchange reactions, they proceeded at a faster rate along the incipient P-layers; the rate increase is thought to be due to the greater passage of fluid along the incipient P-layers. Such a model may be acting independently of or at the same time as pressure solution effects.

13. Even though the Clunes metasediments have only suffered a single deformation event and low-grade metamorphism, it is clear that diffusive processes and growth of new micas are significant and, particularly in the finer grained rocks, obscure the effects of mechanical reorienting processes. However, pore deformation and permeability changes as well as rotation of pre-$S_1$ phyllosilicates, all related to the $D_1$ deformation, are equally important in the formation of $S_1$. It is suggested that, in multiply deformed and/or higher grade rocks elsewhere, it may be

a gross oversimplification to assume that recrystallization and/or grain growth processes are dominant as far as preferred orientation development is concerned; the earlier deformation history involving mechanical reorienting processes, pore shape changes, et cetera may well be making a fundamental contribution to orientation development.

ACKNOWLEDGMENTS

The authors wish to thank Professor E. S. Hills for introducing them to the problem in Victoria; Dr. H. W. Nesbitt for many useful suggestions; Western Mining Corporation, in particular J. H. Lalor and D. R. Quick, for providing access to the drill core and certain financial assistance to MJG; R. Soong of the D.S.I.R. New Zealand for the infrared analyses; and the Australian Institute of Nuclear Science and Engineering for providing support to RRK. The authors wish to acknowledge a Commonwealth (of Australia) Postgraduate Research Award to MJG. Drs. T. P. Hopwood and P. F. Williams are thanked for their comments and criticism of the manuscript. K. Karlsson assisted with the drafting of one of the figures while the manuscript was typed by K. H. Stephens and E. Månsson.

REFERENCES

Allen, J. R. L., and Banks, N. L., 1972, An interpretation and analysis of recumbent-folded deformed cross-bedding: Sedimentology, v. 19, p. 257-283.

Alterman, I. B., 1973, Rotation and dewatering during slaty cleavage formation: some new evidence and interpretations: Geology, v. 1, p. 33-36.

Baragwanath, W., 1917, The Clunes Goldfield: Victoria Geol. Survey Records, v. 4(1), p. 33-35.

Beavis, F. C., 1967, Structures in the Ordovician rocks of Victoria: Royal Soc. Victoria Proc., v. 32, p. 147-182.

———— 1970, Cleavages and linear structures in Ordovician sandstones, Victoria: Geol. Mag., v. 107, p. 429-438.

Cann, J. R., 1970, Rb, Sr, Y, Zr, Nb in some ocean-floor basaltic rocks: Earth Planetary Sci. Letters, v. 10, p. 7-11.

Cloos, E., 1947, Oolite deformation in the South Mountain Fold, Maryland: Geol. Soc. America Bull., v. 58, p. 843-918.

Cohen, M., 1970, Self diffusion during plastic deformation: Japan Inst. Metals Trans., v. 11, p. 145-151.

Coldham, J. C., 1953, Clunes gold mines, *in* Edwards, A. B., ed., Geology of Australian Ore Deposits: Empire Min. Met. Cong., 5th, Melbourne, 1953, p. 1003-1010.

Cosgrove, J. W., 1976, The formation of crenulation cleavage: Geol. Soc. London Jour., v. 132, p. 155-178.

Durney, D. W., 1972, Solution transfer, an important geological deformation mechanism: Nature, v. 235, p. 315-317.

Elliot, D., 1973, Diffusion flow laws in metamorphic rocks: Geol. Soc. America Bull., v. 84, p. 2645-2664.

Etheridge, M. A., Paterson, M. S., and Hobbs, B. E., 1974, Experimentally produced preferred orientation in synthetic mica aggregates: Contr. Mineralogy Petrology, v. 44, p. 275-294.

Gay, N. C., 1969, The analysis of strain in the Barberton Mountain Land, Eastern Transvaal, using deformed pebbles: Jour. Geology, v. 77, p. 377-396.

Glasson, M. J., and Keays, R. R., 1978, Gold mobilization during cleavage development in sedimentary rocks from the auriferous slate belt of Central Victoria, Australia: Some important boundary conditions: Econ. Geology, v. 73, p. 496-511.

Gray, D. R., 1977, Differentiation associated with discrete crenulation cleavages: Lithos, v. 10, p. 89-101.

Green, H. W., Griggs, D. T., and Christie, J. M., 1970, Syntectonic and annealing recrystallization of fine-grained quartz aggregates, *in* Paulitsch, P., ed., Experimental and Natural Rock Deformation: Berlin-Heidelberg, Springer-Verlag, p. 272-335.

Groshong, R. H., 1975, 'Slip'-cleavage caused by pressure solution in a buckle fold: Geology, v. 3, p. 411-413.
Helgeson, H. C., 1967, Solution chemistry and metamorphism, *in* Abelson, P. H., ed., Researches in Geochemistry, v. 2: New York, John Wiley & Sons Inc., p. 362-405.
Helm, D. G., and Siddans, A. W. B., 1971, Deformation of a slaty, lapillar tuff in the English Lake District: Discussion: Geol. Soc. America Bull., v. 82, p. 523-532.
Hills, E. S., 1963, Elements of Structural Geology: London, Methuen, 483 p.
Hills, E. S., and Thomas, D. E., 1954, Turbidity currents and the graptolitic facies in Victoria: Geol. Soc. Australia Jour., v. 1, p. 119-133.
Hossack, J. R., 1968, Pebble deformation and thrusting in the Bygdin area (Southern Norway): Tectonophysics, v. 5, p. 315-339.
Kamb, W. B., 1959, Theory of preferred crystal orientation developed by crystallization under stress: Jour. Geology, v. 67, p.153-170.
Knill, J. L., 1960, A classification of cleavages with special reference to the Craignish district of the Scottish Highlands: Internat. Geol. Cong., 21st, Copenhagen 1960, Rept., pt. 18, p. 317-325.
Lowe, D. R., 1975, Water escape structures in coarse-grained sediments: Sedimentology, v. 22, p. 157-204.
Maxwell, J. C., 1962, Origin of slaty and fracture cleavage in the Delaware Water Gap area, New Jersey and Pennsylvania, *in* Engel, A. E. J., James, H. L., and Leonard, B. F., eds., Petrologic Studies: A Volume in Honor of A. F. Buddington: Boulder, Colo., Geol. Soc. America, p. 281-311.
McKee, E. D., Reynolds, M. A., and Baker, C. H., 1962, Experiments on intraformational recumbent folds in cross-bedded sand: U.S. Geol. Survey Prof. Paper 450-D, p. 155-160.
Means, W. D., and Paterson, M. S., 1966, Experiments on preferred orientation of platy minerals: Contr. Mineralogy Petrology, v. 13, p. 108-133.
Norrish, K., and Hutton, J. T., 1969, An accurate X-ray spectrographic method for the analysis of a wide range of geological samples: Geochim. et Cosmochim. Acta, v. 33, p. 431-453.
Oertel, G., 1970, Deformation of a slaty, lapillar tuff in the Lake District, England: Geol. Soc. America Bull., v. 81, p. 1173-1188.
Paterson, M. S., 1973, Nonhydrostatic thermodynamics and its geologic applications: Rev. Geophysics Space Physics, v. 11, p. 355-390.
Pearce, J. A., 1975, Basalt geochemistry used to investigate past tectonic environments on Cyprus: Tectonophysics, v. 25, p. 41-68.
Plessmann, Von W., 1964, Gesteinslösung, ein Hauptfaktor beim Scheiferungsprozess: Geol. Mitt., v. 4, p. 69-82.
Powell, C. McA., 1969, Intrusive sandstone dykes in the Siamo Slate near Negaunee, Michigan: Geol. Soc. America Bull., v. 80, p. 2585-2594.
Ramsay, J. G., 1967, Folding and Fracturing of Rocks: New York, McGraw-Hill Book Co., 568 p.
Rickard, M. J., 1961, A note on cleavage in crenulated rocks: Geol. Mag., v. 98, p. 324-332.
Singleton, O. P., 1965, Geology and mineralization of Victoria, *in* McAndrew, J., ed., Geology of Australian Ore Deposits: Commonwealth Min. Met. Cong., 8th, Melbourne, 1965, p. 440-449.
Sorby, H. C., 1856, On slaty cleavage, as exhibited in the Devonian limestones of Devonshire: Philos. Mag., v. 11, p. 20-37.
Spry, A. H., 1969, Metamorphic Textures: Oxford, Pergamon Press, 350 p.
Stephens, M. B., 1975, Pebble strain analysis in the Vojtja conglomerate of central Västerbotten, Sweden: Geol. Fören. Stockholm Förh., v. 97, p. 74-82.
Talbot, J. L., and Hobbs, B. E., 1968, The relationship of metamorphic differentiation to other structural features at three localities: Jour. Geology, v. 76, p. 581-587.
Thomas, D. E., 1939, The structure of Victoria with respect to the Lower Paleozoic rocks: Min. Geol. Jour. (Victoria), v. 1(4), p. 59-64.
Voll, G., 1960, New work on petrofabrics: Liverpool-Manchester Geol. Jour., v. 2, p. 503-567.
White, S., 1975, Tectonic deformation and recrystallization of oligoclase: Contr. Mineralogy Petrology, v. 50, p. 287-304.
Williams, P. F., 1972, Development of metamorphic layering and cleavage in low grade metamorphic rocks at Bermagui, Australia: Am. Jour. Sci., v. 272, p. 1-47.
Wilson, C. J. L., 1973, The prograde microfabric in a deformed quartzite sequence, Mount Isa, Australia: Tectonophysics, v. 19, p. 39-81.
Wood, D. S., 1974, Current views of the development of slaty cleavage: Ann. Rev. Earth and Planetary Sci., v. 2, p. 369-401.